International Journal of Research Instinct
(Peer-reviewed Journal)

ISSN ONLINE 2348-2095
Research Article

IMAGE FUSION USING UNDECIAMTED WAVELET TRANSFORM

[1]N. Seeni Fathima ,[2]S. Brundha

[1&2]Asst.professor, Caussanel College of Arts and Science, Muthupettai.

[1].fathimaasmathali@gmail.com,[2].sbruntha12@gmail.com

ABSTRACT

In the image fusion process, two images are taken. The properties in both of the input images are preserved in the resulting image. The fusion process is employed using the wavelet transformation. The wavelet transformation decomposes the images into several components. The low components consist of the low level information in the images. The low components are selected for the fusion of the images. The fusion process is employed by selecting the pixels in the images. The selection of the pixels is done by using optimal pixel that consists of more important information in the images. The performance of the process is measured by calculation of the mean and the standard deviation of the process. Image fusion process helps in producing enhanced image consisting of both the information from the two input images. Multiscale transforms are among the most popular techniques in the field of pixel-level image fusion. The fusion performance of these methods often deteriorates for images derived from different sensor modalities. The wavelet based transformation of the input images helps in preserving the image properties so that the resulting image contains the information present in both the images. The UWT reduces unwanted side effects such as ringing artifacts in the fused image and it gives better results than any other methods.

1. INTRODUCTION

1.1 What Is Image Fusion?

Image Fusion is a process of combining the relevant information from a set of images of the same scene, into a single image, where in the resultant fused image will be more informative and complete than any of the input images. Input images could be multi sensor, multimodal, multifocal or multi temporal. One of the goals of image fusion is to create a single enhanced image more suitable for the purpose of human visual perception, object detection and target recognition.

The source images that can be used are Computed Tomography (CT), Magnetic Resonance Imaging (MRI) and Positron Emission Tomography (PET). A single medical mode of medical image cannot provide accurate and comprehensive information and hence the medical image fusion has become the focus of image research and processing. The process of image fusion can be performed at pixel, feature or decision level.

1.2 Categories Of Image Fusion

We categorize the image fusion methods according to the data entering the fusion and according to the fusion purpose. Input images could be from any of the following categories:

1) Multimodal Images: Multimodal fusion of images is applied to images coming from different modalities like visible and infrared, CT and MRI or panchromatic and multispectral satellite images. The goal of the multimodal image fusion system is to decrease the amount of data and to emphasize band-specific information.

2) Multifocal Images: In applications of digital cameras, when a lens focuses on a subject at a certain distance, all subjects at that distance are not sharply focused. A possible way to solve this problem is by image fusion, in which one can acquire a series of pictures with different focus settings and fuse them to produce a single image with extended depth of field. The goal of this type of fusion is to obtain a single all-in focus image.

3) Multi-view Images: In multi-view image fusion, a set of images of the same scene is taken by the same sensor but from different viewpoints or several 3D acquisitions of the same specimen taken from different viewpoints are fused to obtain an image with higher resolution. The goal of this type of fusion is to provide complementary information from different viewpoints.

4) Multi-Temporal Images: In Multi-temporal image fusion, images taken at different times (seconds to years) in order to detect changes between them are fused together to obtain one single image.

1.3 Undecimated Wavelet Transform

Wavelets are finite duration oscillatory functions with zero average value [1]. They have finite energy. They are suited for analysis of transient signal. The irregularity and good localization properties make them better basis for analysis of signals with discontinuities. Wavelets can be described by using two functions viz. the scaling function f (t), also known as father wavelet and the wavelet function or mother wavelet. Mother wavelet (t) undergoes translation and scaling operations to give self similar wavelet families as given by equation.

$$\psi_{(a,b)}(t)=\frac{1}{\sqrt{a}}\psi\left(\frac{t-b}{a}\right)\text{ , (a, b } \epsilon \text{ R), a > 0}\ldots\ldots\ldots\ldots\ldots\ldots\ldots\ldots\ldots..(1.1)$$

Where ψ-wavelet function and a, b denotes rows and columns. The wavelets-based approach is appropriate for performing fusion tasks for the following reasons:-

(1) It is a multi scale (multi resolution) approach well suited to manage the different image resolutions. It is useful in a number of image processing applications including the image fusion.

(2) The discrete wavelets transform (DWT) allows the image decomposition in different kinds of coefficients preserving the image information. Such coefficients coming from different images can be appropriately combined to obtain new coefficients so that the information in the original images is collected appropriately.

(3) Once the coefficients are merged the final fused image is achieved through the inverse discrete wavelets transform (IDWT), where the information in the merged coefficients is also preserved.

The wavelet transform decomposes the image into low-high, high-low, high-high spatial frequency bands at different scales and the low-low band at the coarsest scale which is shown in fig: 1.1. The L-L band contains the average image information whereas the other bands contain directional information due to spatial orientation. Higher absolute values of wavelet coefficients in the high bands correspond to salient features such as edges or lines.

In common with all transform domain fusion techniques the transformed images are combined in the transform domain using a defined fusion rule then transformed back to the spatial domain to give the resulting fused image.

$$\begin{array}{c} x,y \\ \omega\left(I_1(¿),\omega\left(I_2(x,y)\right)\right) \\ \varnothing ¿ \\ I(x,y)=\omega^{-1}¿ \end{array} \ldots\ldots\ldots\ldots\ldots\ldots(1.2)$$

Wavelet transform fusion is more formally defined by considering the wavelet transforms ω of the two registered input images $I_1(x, y)$ and $I_2(x, y)$ together with the fusion rule $\varnothing$. Then, the inverse wavelet transform ω^{-1} is computed, and the fused image I(x, y) reconstructed. It is denoted by the eqn: 1.2.

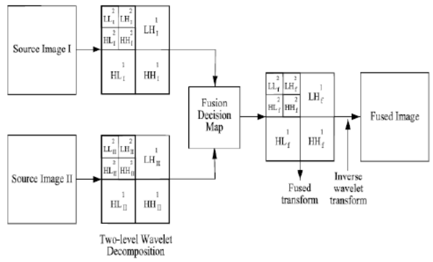

Figure 1.1: Wavelet based image fusion

The decimated (bi) orthogonal wavelet transform is highly used in image compression algorithms such as JPEG-2000, results are far from optimal for other applications such as image fusion. This is mainly due to the down sampling in each decomposition step of the DWT which may cause a large number of artifacts when reconstructing an image after modification of its wavelet coefficients. Thus, for applications such as image fusion, where redundancy is not a crucial factor, performance can be improved significantly by removing the decimation step in the DWT, leading to the non-orthogonal, translate-invariant UWT.

Like the DWT, the undecimated wavelet transform (UWT) is implemented using the filter bank which decomposes an one dimensional (1-D) signal c_0 leads to a set W={w_1…., w_J, c_J} in which w_J represents the high-pass or the wavelet coefficients at scale j and c_J are the low-pass or approximation coefficients at the lowest scale j. The passage from one resolution to the next one is obtained using the "à trous" algorithm, where the analysis low-pass and analysis high-pass filter h and g are upsampled by 2^j when processing the j^{th} scale, where j=0,1,..,J-1. Thus, the UWT decomposition is defined as

$$c_{j+1}[n]=\left(\acute{h}(j)*c_j\right)[n]=\sum_m h[m]\,c_j[n+2^j m] \quad \text{…………..(1.3)}$$

$$w_{j+1}[n]=\left(g(j)*c_j\right)[n]=\sum_m g[m]\,c_j[n+2^j m] \quad \text{………..(1.4)}$$

Where $h^{(j)}[n]$ = h[-n] and $h^{(j)}$ [n]=h[$\frac{n}{2j}$¿ if [$\frac{n}{2j}$¿ is an integer and 0, otherwise. The reconstruction at scale j is obtained by

$$c_j[n]=\frac{1}{2}\left[\left(\acute{h}(j)*cj\right)[n]+\left(g(j)*w_{j+1}\right)[n]\right] \quad \text{………………(1.5)}$$

Where $\acute{h}$ and g are the upsampled low-pass and high-pass synthesis filters, respectively. Perfect reconstruction holds if the used analysis and synthesis filters satisfy the condition

$$H\left(z^{-1}\right)\widetilde{H}(z)+G\left(z^{-1}\right)\widetilde{G}(z)=1 \quad \text{……………………………..(1.6)}$$

In the z-transform domain, which provides additional freedom during the filter selection process compared to the DWT where, in addition to the perfect reconstruction condition, an anti-aliasing condition has to be satisfied as well. The UWT can be extended to 2-D by

$$c_{j+1}[m,n]=\left(\acute{h}(j)\acute{h}(j)*c_j\right)[m,n]$$
$$w^1_{j+1}[m,n]=\left(\acute{h}(j)\acute{g}(j)*c_j\right)[m,n]$$
$$w^2_{j+1}[m,n]=\left(\acute{g}(j)\acute{h}(j)*c_j\right)[m,n]$$
$$w^3_{j+1}[m,n]=\left(\acute{g}(j)\acute{g}(j)*c_j\right)[m,n] \quad \ldots\ldots\ldots\ldots\ldots\ldots\ldots\ldots\ldots(1.7)$$

Where the rows and columns are filtered separately by h and g, leading to three high-pass or detail images w^1 , w^2, w^3 per stage corresponding to the horizontal, vertical and diagonal directions. The redundancy factor of UWT J-level decomposition is 3J+1, since each high-pass image has the same size than the original image.

Since the filters do not need to be (bi)orthogonal, an alternative approach in multispectral image fusion, for example fusion of high-resolution panchromatic images with low resolution multispectral images, is to define g[n]=δ[n]-h[n], where δ[n] represents an impulse at n=0. In 2-D this yields g[m,n] = δ[m,n]-h[m,n], which suggests that the detail images can be obtained by taking the difference between two successive approximation images. A common choice for the analysis, low-pass filter h is a B-spline filter. The implementation of the UWT is known as Isotropic Undecimated Wavelet Transform or Additive Wavelet Transform.[8]

1.4 Proposed System

In multiscale pixel level image fusion, a transform coefficient of an image is associated with a feature if its value is influenced by the features pixel. We will refer to a given decomposition level j, orientation band b, and position m, n of a coefficient as its localization. A given feature from one of the source images is only conserved correctly in the fused image if all associated coefficients are employed to generate the fused multiscale representation. However, in many situations this is not practical since, given a localization I, the coefficient $y_A(I)$ from image I_A may be associated to a feature f_A and the coefficient $y_B(I)$ from image I_B may be associated to a feature f_B . In this case, choosing one coefficient instead of the other may result in the loss of an important salient feature from one of the source images. For example, in the case of a camouflaged person hiding behind a bush the person may appear only in the infrared image and the bush only in the visible image. If the bush has high textural content, this may result in large coefficient values at coincident localizations in both decomposition of an infrared-visible image pair. The fusion rules that choose just one of the coefficients for each localization may introduce discontinuities in the fused sub band signals. These may lead to reconstruction errors such as ringing artifacts or substantial loss of information in the final fused image. It is important to note that the above mentioned problem is aggravated with the increase of the support filters used during the decomposition process.

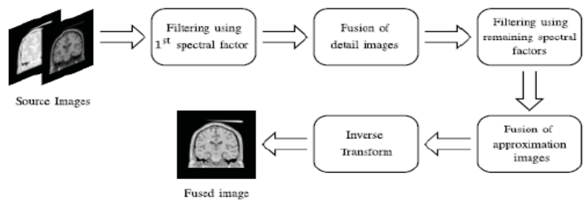

Figure 1.2: Schematic diagram for proposed work.

We propose a novel UWT-based pixel-level image fusion approach, which attempts to circumvent the coefficient spreading problem by splitting the image decomposition procedure into two successive filter operations using spectral factorization of analysis filters. A schematic diagram of the suggested image fusion framework is given in fig: 1.2. The co-registered source images are first transformed to the UWT domain by using very short filter pair, derived from the first spectral factor of the overall analysis filter bank. After the fusion of the high-pass coefficients, the second filter pair, consisting of all remaining spectral factors, is applied to the approximation and fused, detail images. This yields the first decomposition level of the proposed fusion approach. Next, the process is recursively applied to the approximation images at the coarsest scale the inverse transform is applied to the composite UWT representation, resulting in the final fused image.

2. UWT WITH SPECTRAL FACTORIZATION

An input image can be represented in the transform domain by a sequence of detail image at different scales and orientations along with an approximation image at the coarsest scale. Hence, the multiscale decomposition of an input image I_k can be represented as

$$Y_k = \{y_k^{1,} y_k^{2}, \ldots.. y_k^{J}, x_k^{J}\} \quad \ldots\ldots\ldots\ldots\ldots\ldots\ldots\ldots\ldots\ldots\ldots\ldots(2.1)$$

Where the equation 2.1. x_k^J represents the approximation image at the lowest scale J and y_k^J, j=1,2,3,……J represent the detail images at level j. These are comprised of various orientation bands. Thus, $y_k^j[n,p]$ represent the detail coefficient of input image k, at location n, within decomposition level j and orientation band p. That the fused image will be generated from two source images I_A and I_B which are assumed to be registered prior to the fusion process.[13]

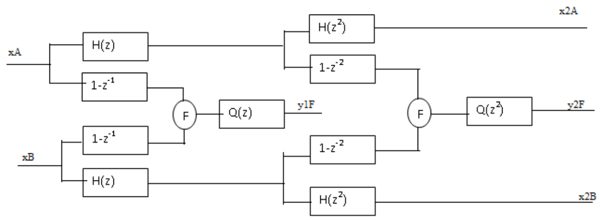

Figure 2.1: Spectral factorization for two decomposition levels.

Whereas the highly redundant UWT, DTCWT and NSCT are invariant to shifts occurring in the input images, the DWT represent shift-variant transforms with no or limited redundancy. The redundancy and shift-invariance are desirable properties in image fusion applications since they allow for a higher robustness to rapid changes in coefficient values, thus, reducing the amount of reconstruction errors in the fused image. The filters with large support size may result in an undesirable spreading of coefficient values which, in case of salient features located very close to each other in both input images, may lead to coefficients with coincident localizations in the transform domain. Since it is difficult to resolve such overlaps, distortions may be introduced during the fusion process, such as artifacts or even loss of transformation. The multi sensor images and especially medical image pairs often exhibit similar properties. Hence, for these images the fusion performance considerably degrades with an increase of the filter size. We can therefore reduce the problem of choosing a proper redundant multiscale transform to its ability to incorporate a filter bank with a sufficiently small support size, thus, minimizing the coefficient spreading problem. From this point of view, the UWT appears to be an attractive choice due to the standard tensor product construction in 2-D, the UWT offers directionality without increasing the overall length of the implemented filter bank a property not shared by the NSCT and DTCWT. We propose a novel UWT-based fusion approach that splits the filtering process into two successive filtering operations and performs the actual fusion after convolving the input signal with the first filter pair, exhibiting a significantly smaller support size than the original filter.[3]

The proposed method is based on the fact that the low-pass analysis filter H(z) and the corresponding high-pass analysis filter G(z) can always be expressed in the form

$$H(z) = (1+z^{-1})\,P(z) \quad \ldots\ldots\ldots\ldots\ldots\ldots\ldots\ldots\ldots\ldots\ldots\ldots\ldots\ldots\ldots (2.2)$$

$$G(z) = (1-z^{-1})\,Q(z) \quad \ldots\ldots\ldots\ldots\ldots\ldots\ldots\ldots\ldots\ldots\ldots\ldots\ldots\ldots\ldots (2.3)$$

The Figure 2.1 depicts spectral factorization in the z-transform domain. Thus, in our framework the input images are first decomposed by applying a spectral, represented by the first spectral factors $(1+z^{-1})$ and $(1-z^{-1})$ respectively as given by the equation 2.2 and 2.3.

The resulting horizontal, vertical and diagonal detail images can afterwards be fused according to an arbitrary fusion rule. Next, the filter pair represented by the second spectral factor P(z) and Q(z) in the above equation is applied to the approximation and fused detail images, yielding the first decomposition level of the proposed fusion scheme. For each subsequent level, the analysis filters are upsampled according to the "a trous" algorithm, leading to the following, generalized analysis filter bank

$$H(z^{2j-1}) = (1+z^{-2j-1})\,P(z^{2j-1}) \quad \ldots\ldots\ldots\ldots\ldots\ldots\ldots\ldots\ldots\ldots\ldots(2.4)$$

$$G(z^{2j-1}) = (1-z^{-2j-1})\,Q(z^{2j-1}) \quad \ldots\ldots\ldots\ldots\ldots\ldots\ldots\ldots\ldots\ldots\ldots(2.5)$$

and the aforementioned procedure is recursively applied to the approximation images, until the desired number of decomposition levels is reached. After merging the low-pass approximation images, the final image is obtained by applying the inverse transform, using the corresponding synthesis filter bank with spectral factorization.[11]

2.1 Filter Bank Design

Due to the nonsubsampled nature of the UWT, many ways exist to construct the fused image form its wavelet coefficients. For a given analysis filter bank (h ,g), any synthesis filter bank ($\tilde{h},\tilde{g}$¿ satisfying the perfect reconstruction condition of eq.(1.6) can be used for reconstruction.

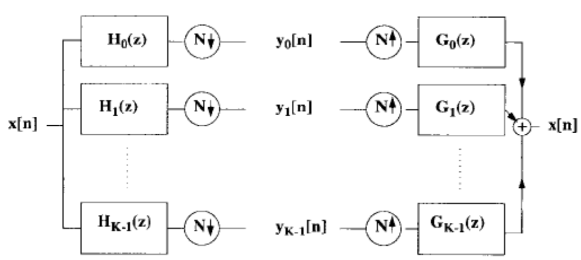

(a) (b)

Figure: 2.2 (a) analysis filter bank and (b) synthesis filter bank

The polyphase analysis matrix of a nonsubsampled filter bank see Fig: 2.2(a) is a column vector whose entries are the analysis filters themselves

$$H(z) = [H_0(z)\ H_1(z) \ldots\ldots H_{k-1}(z)]^T \quad \ldots\ldots\ldots\ldots\ldots\ldots\ldots\ldots\ldots\ldots\ldots(2.6)$$

perfect and stable reconstruction is possible, provided that there exist stable filters $G_0(z)\ G_1(z)\ldots\ldots G_{k-1}(z)$ such that

$$H_0(z)\ G_0(z) + H_1(z)\ G_1(z) + \ldots\ldots + H_{k-1}(z)\ G_{k-1}(z) = 1 \ldots\ldots\ldots\ldots\ldots (2.7)$$

The reconstruction is performed by a synthesis filter bank with the filters $G_i(z)$[19]. Nonsubsampled filter banks have several nice properties. Constraints for perfect reconstruction are mild and allow for very flexible design. The highly redundant representations they generate can be close discrete-time approximations of continuous-time transforms. Examples of applications for which that property is crucial are applications based on wavelet modulus maxima representations, which are proposed by Mallat *et al.* for singularity detection, signal denoising and compression, and which use nonsubsampled filter banks as the preprocessing tool. The standard three directional UWT can be obtained by expanding the filter bank to 2-D. This approach has some interesting characteristics. For example, due to the lack of convolutions during reconstruction, no additional distortions are introduced when constructing the fused image. Since, the fused image can be obtained by a simple co-addition of all detail images and the approximation image, a very fast reconstruction is possible. On the other hand, distortions introduced during the fusion process remain unfiltered in the reconstructed image. Additionally, distortions introduced during the fusion stage are not transferred unprocessed to the reconstructed image as in the standard case where only summations are involved during reconstruction.

Nonsubsampled filter banks also find their place in applications that require shift-invariant representations, a requirement that conflicts with subsampling in the filter bank channels. The nonsubsampled filter banks are not only convenient for implementation in discrete time but also give rise to a broad spectrum of wavelets that can be derived from iterated octave band trees. Note that for singularity detection and discrimination, it is important to use wavelets with a given number of vanishing moments and a certain high degree of regularity.

3. Fusion Rules

Choose Max (CM)

The first investigated combination scheme is the simple "choose max" (CM) or maximum selection fusion rule. By this rule the coefficient yielding the highest energy is directly transferred to the fused decomposed representation. Hence, for each decomposition level j, orientation band p and location n, the fused, detail images y^j_F are defined as

$$\begin{cases} y_A^j[n,p] & \text{if } |\,y_A^j[n,p]| > |\,y_B^j[n,p]| \\ \end{cases}$$

$y_F^j[n,p] = \quad y_B^j[n,p] \quad \text{otherwise}$ ……..……(3.1)

The choice is motivated by the fact that salient features, such as edges, lines or other discontinuities, result in large magnitude coefficients, and thus can be captured using this combination scheme.

Choose Max with Intra Scale (CM-IS)

The simple CM fusion rule does not take into account that, by construction, each coefficient within a multiscale decomposition is related to a set of coefficients in other orientation bands and decomposition levels. Hence, in order to conserve a given feature from one of the source images, all the coefficients corresponding to it have to be transferred to the composite multiscale representation as well. One way to improve the fusion results is therefore the use of intra scale grouping in combination with the CM fusion scheme of eq.(3.1).

$$y_F^j[n,p] = \begin{cases} y_A^j[n,p] & \text{if } \sum |y_A^j[n,p]| > |\sum y_B^j[n,p]| \\ y_B^j[n,p] & \text{otherwise} \end{cases} \quad \text{..……(3.2)}$$

Since the combination schemes of above equations suffer from a relative low tolerance against noise which may lead to a salt and pepper appearance of the selection maps, robustness can be added to the fusion process using an area based selection criteria.

Choose Max Activity (CM-A)

Since the combination schemes of equations (3.1) and (3.2) suffer from a relative low tolerance against noise which may lead to a salt and pepper appearance of the selection maps, robustness can be to the fusion process using an area based selection criteria[10]. We expand the CM-IS combination scheme of above fusion rule: Calculate the activity a_k^j of each coefficient as the energy within a 3*3 window W centered at the current coefficient position n and select the coefficient which yields the highest activity, again, by considering the intra-scale dependencies between coefficients from different orientation bands.

$$a_k^j [n,p] = \sum | y_k^j [n+\Delta n, p]|^2 \quad \text{…………………………………..(3.3)}$$

$$y_F^j[n,p] = \begin{cases} y_A^j[n,p] & \text{if } \sum a_A^j[n,q] > \sum a_B^j[n,q] \\ y_B^j[n,p] & \text{otherwise} \end{cases} \quad \text{…….(3.4)}$$

However, this assumption is not always valid and a fusion rule which uses a weighted combination of the transform coefficients may give better results.

Choose Max Activity Measure (CM-AM)

We implement as the fourth fusion rule, a modified version of one given by Burt and Kolczynski. In their approach a match measure m_{AB}^{j} is calculated which is used to determine the similarity between the transformed source images.

$$m_{AB}^{j}[n,p] = \frac{2\sum y_{A}^{j}[n+\Delta n, p]\, y_{B}^{j}[n+\Delta n, p]}{a_{A}^{j}[n, p] + a_{B}^{j}[n, p]} \quad \ldots\ldots\ldots\ldots\ldots\ldots(3.5)$$

where W is a 3*3 window centered at n and a_{k}^{j} is the activity measure of eq.(3.4). The fused coefficients y_{F}^{j} are given by the weighted average.

$$y_{F}^{j}[n,p] = w_{A}^{j}[n, p]\, y_{A}^{j}[n, p] + w_{B}^{j}[n, p]\, y_{B}^{j}[n, p] \quad \ldots\ldots\ldots\ldots(3.6)$$

The low-pass approximation images will be treated differently by our combination schemes. Unlike the case of the detail images, high magnitudes in the approximation images do not necessarily correspond to important features within the source images [13]. Classically, filter banks comprise of a series of band pass filters. Non-critical decimation of the resulting subbands will permit the benefit of lower computational complexity while avoiding aliasing in the subbands, which would otherwise limit the performance of, for example, adaptive filters operating independently on the various subband signals. In the literature more sophisticated and effective approximation fusion rules can be found. These rules have little influence on the overall fusion performance. Additionally, our proposed fusion framework does not suggest any improvements regarding the fusion of the approximation images eq. (3.6) will suffice for the assessment of our method.

4. PERFORMANCE ANALYSIS

The general requirements of an image fusing process are that it should preserve all valid and useful pattern information from the source images, while at the same time it should not introduce artifacts that could interfere with subsequent analyses. The performance measures used in this paper provide some quantitative comparison among different fusion schemes, mainly aiming at measuring the definition of an image[4]. Performance measures are used essential to measure the possible benefits of fusion and also used to compare results obtained with different algorithms. Mean is the representative value of a large dataset that describes the center or middle value. Mean is the measure of the group contributions per contributor which is conceived to be the same as the amount contributed by each *n* contributor if each to contribute equal amounts. Mean represents brightness and standard deviation represents contrast of image.

$$\acute{x}=\frac{1}{n}\sum_{i=1}^{n} x_i \quad \ldots\ldots\ldots\ldots\ldots\ldots\ldots\ldots\ldots\ldots\ldots(4.1)$$

Standard Deviation provides a way to determine regions which are clear and vague. It is a most widely used measure of variability or diversity used in statistics. In terms of image processing it shows how much variation or "dispersion" exists from the average (mean, or expected value). A low standard deviation indicates that the data points tend to be very close to the mean, whereas high standard deviation indicates that the data points are spread out over a large range of values. It is calculated by the formula

$$s=\sqrt{\frac{1}{n}\sum_{i=1}^{n}\left(x_i-\acute{x}\right)^2} \quad \ldots\ldots\ldots\ldots\ldots\ldots\ldots(4.2)$$

Where $\acute{x}=\frac{1}{n}\sum_{i=1}^{n} x_i$

Standard Deviation is calculated on the low frequency components of the input images within a 3- by-3 window and whichever having higher values of mean are selected as the fusion coefficients among the low frequency components.

5. RESULTS AND DISCUSSIONS

In this work, I have used the qualitative methods for analysis the results. The qualitative methods are acceptance and verification tests which are accepted or rejected by a possible user, which determine visually the relative perceived image quality based on the contribution that the fusion makes to its specific problem. The experiments are organized to apply four fusion algorithms with image quality measure mean and standard deviation by using three types of imagery.

As the optical lenses in CCD devices have limited depth-of focus, it is often impossible to obtain an image in which all relevant objects are in focus. To achieve all interesting objects in focus, several CCD images, each of which contains some part of the objects in focus, are required[6]. I have successfully fused MRI and CT images to create a single fused image, providing a new and effective combined modality for diagnosis. In the figure:5.1 (c) show the UN camp visual and IR source images, and the fused image. It is observed from the fused images that the proposed method is able to transfer the fine details present in the visible image to the fused image.

The fusion process is expected to select all focused objects from these images. The performance of the proposed UWT fusion scheme with spectral factorization is compared to the results obtained by applying the Haar, Spline, LeGall 5/3, CDF 9/7. As for the objective assessment of multiscale image fusion, a considerable number of evaluation metrics can be found in the literature[3]. These metrics consider only the input images and the fused image to produce a single numerical score that indicates the success of the fusion process. In this work I used mean and standard deviation fusion metrics to evaluate the achieved results.

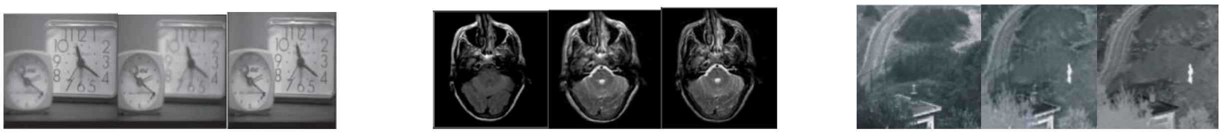

Figure 5.1 (a)Multifocus Images (b) Medical Images (c) Infra red/visible Images

Comparative analysis of Fusion results for multifocus,medical and infrared image pairs:

Transform	**Mean**	**Standard deviation**	**Transform**	**Mean**	**Standard deviation**	**Transform**	**Mean**	**Standard deviation**
Haar	0.731497	0.052664	Haar	0.710046	0.044115	Haar	0.594900	0.073936
Spline	0.721410	0.056259	Spline	0.693701	0.043084	Spline	0.581765	0.073912
LeGall 5/3	0.732346	0.052705	LeGall 5/3	0.692190	0.041951	LeGall 5/3	0.588013	0.069352
CDF 9/7	0.726155	0.055670	CDF 9/7	0.682741	0.043217	CDF 9/7	0.586508	0.068751
Sym4	0.742644	0.054017	Sym4	0.725089	0.045002	Sym4	0.603815	0.074251

Table 5.1: Fusion results for multifocus, medical and infrared image pairs.

6. CONCLUSION

The proposed method utilizes the Undecimated Wavelet Transform to get the two-scale representations, which is simple and effective. More importantly, the transformation of the input pixels is used in a novel way to make full use of the strong correlations between neighborhood pixels for weight optimization. Experiments show that the proposed method can well preserve the original and complementary information of multiple input images. Encouragingly, the proposed method is very robust to image registration. Furthermore, the proposed method is computationally efficient, making it quite qualified for real applications. This paper presents a fast and effective image fusion method for creating high quality fused images by merging component images. The process is employed to different types of images like multi focus, medical and infra-red images. For all the types of the images the fusion process is employed using the four fusion rules. The performance is analysis based on the calculation of the mean and the standard deviation values in the images. The comparisons are listed out in a table.

7. REFERENCES

[1] Aglika Gyaourova, "Undecimated wavelet transforms for image de-noising", Center for Applied Scientific Computing, Lawrence Livermore National Laboratory, November 19, 2002.

[2] A. L. daCunha, J.Zhou and M.N.Do, "The nonsubsampled contourlet transform: Theory, design, and applications", IEEE Transactions on Image Processing, vol. 15, no. 10, pp. 3089–3101, October 2006.

[3] A. Ellmauthaler, E. A. B. da Silva and C. L. Pagliari, "Multiscale Image Fusion Using the Undecimated Wavelet Transform With Spectral Factorization and Non-Orthogonal Filter Banks", IEEE Transactions on Image Processing, 2013.

[4] Fazal-E-Malik, **"**Mean and standard deviation features of color histogram using Laplacian filter for content-based image retrieval", Journal of Theoretical and Applied Information Technology, 15th December 2011. Vol. 34 No.1

[5] Gang Xiao, Kun Wei and Zhongliang Jing, "Improved dynamic image fusion scheme for infrared and visible sequence Based on Image Fusion System", Institute of Aerospace Science and Technology, Shanghai Jiaotong University

[6] Gonzalo Pajares, Jesus Manuel de la Cruz, "A wavelet-based image fusion tutorial" Dpto, Arquitectura de Computadores Automatica, Facultad de Ciencias Fsicas, Universidad Complutense de Madrid, Ciudad Universitaria, 28040 Madrid, Spain, 22 March 2004

[7] Jean-Luc Starck, Jalal Fadili, and Fionn Murtagh "The Undecimated Wavelet Decomposition and its Reconstruction", IEEE Transactions on image processing, Vol. 16, No. 2, February 2007 297-309

[8] S. Li, B. Yang, and J. Hu, "Performance comparison of different multiresolution transforms for image fusion", Information Fusion, vol. 12, no. 2, pp. 74–84, 2011.

[9] María González-Audícana, José Luis Saleta, Raquel García Catalán, and Rafael García, "Fusion of Multispectral and Panchromatic Images Using Improved IHS and PCA Mergers Based on Wavelet Decomposition", IEEE Transactions on Geoscience and Remote sensing, VOL. 42, NO. 6, June 2004.

[10] Melkamu H. Asmare, Vijanth S. Asirvadam, Lila Iznita and Ahmad Fadzil M. Hani "Image Enhancement by Fusion in Contourlet Transform" International Journal on Electrical Engineering and Informatics - Volume 2, Number 1, 2010

[11] Michel Misiti, Yves Misiti, Georges Oppenheim and Jean-Michel Poggi
"Wavelet Toolbox User's Guide" , The mathworks,Inc,2015.

[12] Neethu K, "Image Fusion With Undecimated Wavelet Transform" IJRIT International Journal of Research in Information Technology, Volume 2, Issue 6, June 2014, Pg: 360-363

[13] Paul Hill, Nishan Canagarajah and Dave Bull,"Image Fusion Using Complex Wavelets", vol.40, no.8,pp.400-402, (2004)

[14] Qi Wei, Jos´e Bioucas-Dias, Nicolas Dobigeon, and Jean-Yves Tourneret, "Hyperspectral and Multispectral Image Fusion
based on a Sparse Representation" , Technical Report – 2014, October
University of Toulouse, IRIT/INP-ENSEEIHT

[15] Rakesh M.R, Ajeya B, Mohan A.R , "Hybrid Median Filter for Impulse Noise Removal of an Image in Image Restoration", International Journal of Advanced Research in Electrical, Electronics and Instrumentation Engineering, Vol. 2, Issue 10, October 2013

[16] Rati Khandelwal and S. S. Bedi, "Comprehensive and Comparative Study of Image Fusion Techniques", International Journal of Soft Computing and Engineering (IJSCE) ISSN: 2231-2307, Volume-3, Issue-1, March 2013

[17] I. W. Selesnick, R. G. Baraniuk, and N. C. Kingsbury, "The dual-tree complex wavelet transform," IEEE Signal Processing Magazine, vol.22, no. 6, pp. 123–151, November 2005.

[18] Yong Yang1, Shuying Huang2, Junfeng Gao3, Zhongsheng Qian "Multi-focus Image Fusion Using an Effective Discrete Wavelet Transform Based Algorithm", Measurement Science Review, Volume 14, No. 2, 2014

[19] Zoran Cvetkovi´c and Martin Vetterli "Oversampled Filter Banks" IEEE Transactions on signal processing, VOL. 46, NO. 5, MAY 1998 1245-1255.